Polypropylene/Clay Nanocomposites: Effect of Different Clays and Compatibilizers on Their Morphology

Humberto Palza,[1,2] Rodrigo Vergara,[2] Mehrdad Yazdani-Pedram,[2,3] Raúl Quijada[1,2]

[1]*Departamento de Ingeniería Química y Biotecnología, Facultad de Ciencias Físicas y Matemáticas, Universidad de Chile, Beauchef 861, Santiago, Chile*
[2]*Centro para la Investigación Interdisciplinaria Avanzada en Ciencias de los Materiales (CIMAT), Universidad de Chile, Av. Blanco Encalada 2008, Santiago, Chile*
[3]*Departamento de Química Orgánica y Fisicoquímica, Facultad de Ciencias Químicas y Farmacéuticas, Universidad de Chile, Olivos 1007, Santiago, Chile*

Received 27 March 2008; accepted 6 October 2008
DOI 10.1002/app.29585
Published online 30 January 2009 in Wiley InterScience (www.interscience.wiley.com).

ABSTRACT: A set of organically modified clays (OLS) were mixed with different compatibilizers to alter their interactions with either homopolymer or heterophasic polypropylenes when they were melt-mixed, and the relation between the OLS/compatibilizer system and the composite morphology was studied. X-ray diffraction (XRD) showed that depending on the specific OLS/compatibilizer system, it is possible to obtain several morphologies in the composites. In particular, some samples prepared with compatibilizers based on itaconic acid and OLSs, which had the highest cation exchange capacity and were organically modified with a set of quaternary ammonium salts, presented longer clay interlayer distances than the original OLSs, whereas other composites showed a clay collapse associated with shorter interlayer distances. Moreover, some composites presented both kinds of morphologies together. By means of diffuse reflectance spectroscopy and thermogravimetric analysis, it was possible to show that the OLSs were stable under the operating conditions, so the decrease in the interlayer distance found in some samples was not related to degradation processes. On the other hand, high-resolution transmission electron microscopy (HR-TEM) showed that collapsed clays were formed by tactoid and immiscible structures with poor dispersion in the polymer matrix. However, samples with intercalate state from XRD presented very well dispersed multilayer stacks about 10 nm thick. Finally, those samples with both collapsed and intercalate morphologies presented tactoid and immiscible structures together with well dispersed multilayer stacks in the corresponding HR-TEM images. © 2009 Wiley Periodicals, Inc. J Appl Polym Sci 112: 1278–1286, 2009

Key words: degradation; nanocomposites; structure-property relations; poly(propylene); (PP); clay

INTRODUCTION

Addition of nanoparticles to polymer matrices is one of the recent methods used to develop new plastic composites.[1–3] These nanofillers may be carbon nanotubes,[4] inorganic particles,[5] natural nano-organic compounds,[6] etc. In particular, polymer/layered silicate nanocomposites based on montmorillonite (MMT) are good examples because they allow polymer properties to be improved at reduced cost.[7,8] However, the desired property changes will depend on the final morphology of the filler in a polymer matrix.[9] In this way, only by controlling particle morphology will it be possible to improve some properties at levels similar to those predicted by some theories.[10]

In the particular case of clays, the relation between the filler's morphology and composite properties is even more complicated, because the initial state of the filler is micrometric instead of nanometric, and only a good interaction between a polymer and the clay will be able to produce nanostructured composites.[7,8,11] In this way, to make MMT miscible with polymers one must exchange its alkali counterions with cationic surfactants such as alkylammonium compounds to obtain organically modified layered silicates (OLS).[12] Depending on the strength of the interfacial interactions between a polymer matrix and the layered silicate, three different types of nanocomposites are thermodynamically achievable[7]: (1) tactoid or immiscible, which means that no interaction between the clay and the polymer occurs and no change is seen in the clay's interlayer distance; (2) intercalated, in which the insertion of a polymer matrix into the layered silicate structure occurs in a crystallographically regular fashion and the gallery

Correspondence to: H. Palza (hpalza@ing.uchile.cl).
Contract grant sponsor: FONDAP (CONICYT); contract grant number: 11980002.
Contract grant sponsor: FONDECYT (CONICYT); contract grant number: 1090260.
Contract grant sponsor: FONDECYT INICIACION EN INVESTIGACION (CONICYT); contract grant number: 11075001.

distance increases; and (3) exfoliated, which means that the individual clay layers are separated in a continuous polymer matrix and the interlayer order is disrupted. Whether an admixture of polymer and OLS produces either an exfoliated/intercalated nanocomposite or a conventional microcomposite will depend critically on their characteristics. With respect to polyolefins, it has been shown that by using a compatibilizer such as a polypropylene grafted with maleic anhydride it is possible to prepare clay-based nanocomposites by the melt-mix method.[13,14] So the final morphology will be given by the specific interactions between an OLS, a compatibilizer, and a polymer.

Although polyolefin/clay composites are well known today and it is possible to find a large number of references on this subject, more experimental data are necessary to have a complete understanding of their morphology. For example, it is well accepted that the presence of both compatibilizers and polyolefins increases the clay's interlayer distance.[7,13–15] However, it has been reported that sometimes the opposite is found, which means that the interlayer distance decreases and the clay collapses.[16,17] Yoon et al. have found this behavior in polystyrene/clay nanocomposites, and it was associated with some instabilities of the intercalated organic compounds, generating an arrangement of the alkyl chains from a bilayer to a monolayer structure during processing.[18] On the other hand, Pozsgay et al. also found a clay collapse, but in polypropylene nanocomposites.[19] They suggested that it could be due either to the degradation of organic compounds or to the evaporation of the water molecules present in the clay interlayers. These hypotheses are supported by several publications, because it has been shown that the organic molecules[20–22] coming from OLSs, normally alkyl ammonium salts, decompose by the Hofmann mechanism under the operating conditions (around 200°C) normally used for the polypropylene melt process.[23] However, sufficient proof is missing to support some of the latest explanations.[19]

The present work shows the results of polypropylene nanocomposites prepared by the melt-mix method using a set of different OLSs. Moreover, because the compatibilizer also has a key role in the interactions between a polymer and a clay, three different compatibilizers were studied for each of the OLSs used to evaluate their importance in the final results. The idea is to show that the OLS/compatibilizer system, as a whole, affects the morphology of the composites obtained in a better way than the OLS itself. In a future contribution we will report the relation between the morphologies found and some composite properties.

EXPERIMENTAL

Materials

Montmorillonite samples from three different sources were used: Cloisite 20A from Southern Clay Products, KSF from Aldrich, and a sample from a Chilean producer, Zl, which is a sodium montmorillonite clay from natural volcanic sources in the south of Chile. Cation exchange capacity (CEC) was determined as 55, 80, and 95 [meq/100 g of clay] for KSF, Zl, and Cloisite 20A, respectively. The KSF and Zl clays were modified with octadecylamine (ODA) from Aldrich and were designated as O-KSF and O-Zl, respectively. The particle sizes ($d_{50\%}$) of the different OLSs were 18, 6.7, and 12 μm, respectively, for O-KSF, O-Zl, and Cloisite 20A, measured by a Malvern Mastersizer X instrument. On the other hand, three different compatibilizers were used: one commercial polypropylene grafted with maleic anhydride from Aldrich (PP-*g*-MA) with 0.6 mol % content, and two polypropylenes grafted with either 0.7 mol % or 1.8 mol % of itaconic acid synthesized in our laboratory through a free radical melt reaction process, designated as PPgIA0.7 and PPgIA1.8, respectively.[24,25] A commercial heterophasic polypropylene (HPP) from Petroquímica Cuyo (Argentina) with a melt flow rate of 0.8 g/min, and a homopolymer polypropylene (PP) from Petroquim (Chile) with a melt flow rate of 26 g/min, were used as polymer matrices.

Clay intercalation

A 5-g sample of clay, either KSF or Zl, was dispersed in 500 mL of water using a homogenizer. A solution of 2.1 g of ODA was made at 60°C in a 50 : 50 v/v water : ethanol mixture; it was acidified to pH 3 by adding 2 mL of concentrated hydrochloric acid, and the resulting suspension was then added to the amine solution and stirred vigorously for 2 h at 25°C. The organically modified clays were recovered by filtration, washed abundantly with water, filtered, and then dried at 80°C. The organophilic clays obtained were characterized by XRD and FTIR. Cloisite 20A has a set of quaternary ammonium salts based on hydrogenated tallow of different sizes and it was used as received.

Composite preparation

First, a master batch consisting of a mixture of an organic-modified clay and a compatibilizer in a 1 : 3 clay/compatibilizer weight ratio was prepared by a melt-mixing technique in a Brabender plasticorder internal mixer. The mixing conditions were 190°C, 110 RPM, and 10 min. The composites were also prepared using the Brabender plasticorder, under the

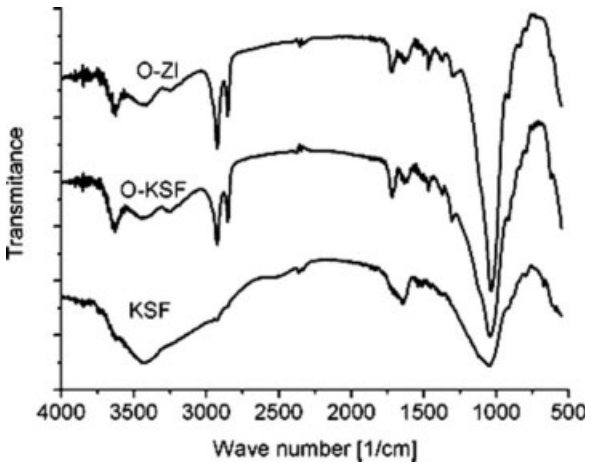

Figure 1 FTIR spectrum of the KSF natural clay and the organically modified clays O-KSF and O-Zl.

same conditions as those used for the preparation of the master batch, by mixing predetermined amounts of the master batch, antioxidant, and neat polymer under a nitrogen atmosphere to obtain nanocomposites containing between 1 and 5 wt % of clay.

Clay and nanocomposite characterization

The clay's interlayer distance was characterized by X-ray diffraction (XRD) using a Siemens D-5000 diffractometer with CuKα = 1.54 Å and a step scan of 0.02° at room temperature. For some samples, its configuration was changed to decrease the lowest angle to 0.7°. The interlayer structure of the OLSs was examined in a Bruker Vector 22 FTIR spectrometer with 100 scans at a resolution of 4 cm^{-1} using KBr for dilution. Diffuse reflectance was measured on the same equipment using a DRIFT accessory with temperature control under a nitrogen atmosphere. The samples were analyzed without any dilution in KBr. Thermogravimetric analysis (TGA) was carried out in nitrogen from room temperature to 600°C in a TA Instruments at a heating rate of 20°C/min. Finally, transmission electron microscopy (TEM) measurements were made on a Philips model CM 100 instrument at 80 kV. HR-TEM images were made on a JEOL-2100F microscope at 200 kV. Ultrathin sections of about 70 nm were obtained by cutting the samples with an Ultracut Reichert-Jung microtome equipped with a Diatome diamond knife.

RESULTS AND DISCUSSION

Organic modification of clays

FTIR analysis was used to evaluate the presence of ODA in both the KSF and the Zl clays. Figure 1 shows the FTIR spectra of neat KSF and O-KSF and O-Zl clays; the typical spectrum of a natural montmorillonite is seen.[26] There is a strong absorption band between 3700 and 3200 cm^{-1} due to the presence of water, another absorption band at 1650 cm^{-1} due to the ν_2(H—O—H) bending vibrations of water molecules, and a strong band at 1050 cm^{-1} due to the Si—O stretching and bending. On the other hand, the presence of organic molecules in both O-KSF and O-Zl is confirmed mainly by the absorption bands at 2922 and 2843 cm^{-1} corresponding to $\nu_{as}(CH_2)$ and $\nu_s(CH_2)$, respectively, which are associated with the C—H stretching of alkylammonium cations.[26] The characteristic δ_{as}(C—H) bending vibration of the $(CH_3)_4N^+$ at 1470 cm^{-1} also appears. The low amount of water in the OLSs is also clear, due to the adsorption of organic cations.[26] The incorporation of organic molecules is also shown by XRD, where it is possible to see the increase of the interlayer distance from 1.23 nm (2θ = 7.2°) to 1.73 nm (2θ = 5°) for O-KSF and from 1.39 nm (2θ = 6.4°) to 2.16 nm (2θ = 4.1°) for O-ZL. Although the same organic modifier was used, the interlayer distance of O-KSF is lower than that of O-Zl. This difference is explained by the higher CEC value of O-Zl. It has been reported that the clay gallery height decreases by decreasing the chain packing density or increasing the available surface area per guest molecule, parameters that are related to the CEC value.[27,28] Although the lateral size of the clay could also be relevant, it has been reported that differences in CEC values are more important.[28] The interlayer distance of Cloisite 20A is 2.47 nm (2θ = 3.5°), which is greater than that in O-Zl in spite of the similar CEC value, and it is associated with the different organic modifiers used.

Nanocomposite structure

XRD was used to analyze the morphology of the master-batches prepared using different compatibilizers and clays, and Figure 2 shows the results for

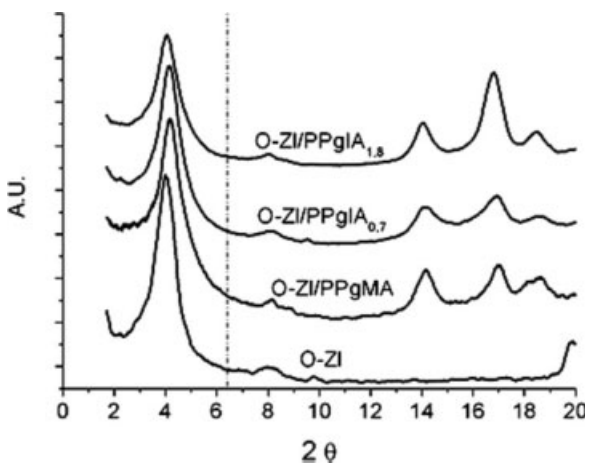

Figure 2 XRD patterns of the O-Zl clay and its master batches with different compatibilizers. The dashed line shows the position of the original peak of the Zl clay.

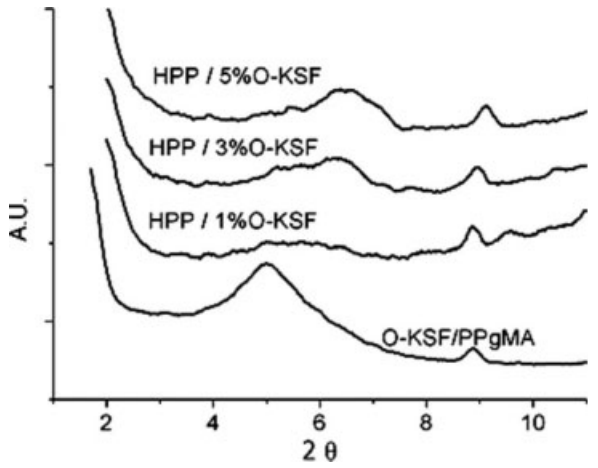

Figure 3 XRD patterns of the O-KSF/PPgMA master batch (adjusted scale) and its composites with HPP for a clay content of 1, 3, and 5 wt %.

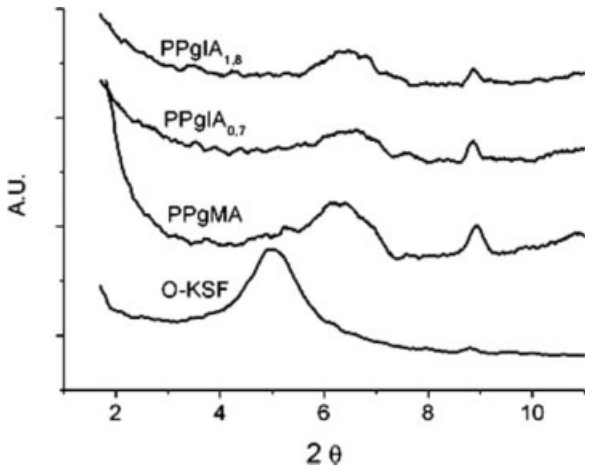

Figure 4 XRD patterns of the HPP/O-KSF composites containing 5 wt % of clay with different types of compatibilizers. The O-KSF clay is also shown for comparison (adjusted scale).

O-Zl. The results for Cloisite 20A and O-KSF are not shown because the same trend was found as for O-Zl. Although it has been reported that when an OLS is mixed with a compatibilizer its interlayer distance increases,[13,14] these samples did not show any important change in the position of the diffraction peaks. Indeed, in the master batches of O-KSF/PPgIAs, the peaks become broader and are displaced to shorter interlayer distances.

On the other hand, as mentioned in the experimental part, the polypropylene/clay nanocomposites were prepared by mixing the master-batch with the neat polymer. The results for the composites based on the high molecular weight heterophasic polypropylene (HPP) using either 1 wt %, 3 wt %, or 5 wt % of the O-KSF with PPgMA as compatibilizer are shown in Figure 3. Contrary to what was expected, the position of the d_{001} peak does not change to smaller angles but is rather shifted to larger ones. So, with the incorporation of the HPP, and regardless of the amount of O-KSF, the clay's interlayer distance decreases, showing clay collapse. It has been reported that the clay intercalation/exfoliation process is more difficult when high molecular weight polypropylenes are used as matrix. The same trend was seen when heterophasic polypropylenes of different molecular weights and morphologies were studied,[29,30] so our results are in agreement with these findings.

With respect to the effect of the compatibilizer, Figure 4 shows the XRD patterns of the HPP composites containing 5 wt % of O-KSF for the three compatibilizers studied. It is clearly seen that regardless of the compatibilizer used, the HPP/O-KSF composites show clay collapse, and their clay interlayer distance decreases from 1.73 nm ($2\theta = 5°$) to 1.35 nm ($2\theta = 6.4°$) for the three compatibilizers tested. A similar behavior was found when 5 wt % of O-Zl was added to the HPP, and in this case the clay interlayer distance decreases from 2.16 nm ($2\theta = 4.1°$) to 1.4 nm ($2\theta = 6.3°$). However, when the HPP/Cloisite 20A composites were analyzed a different trend was found, as can be seen in Figure 5. In particular, it seems that when Cloisite 20A was mixed with HPP, three different morphologies occurred depending on the compatibilizer used. When PPgMA was used, the clay collapsed and its interlayer distance decreased from 2.47 nm ($2\theta = 3.5°$) to 1.85 nm ($2\theta = 4.9°$). The opposite was found when $PPgIA_{1,8}$ was used, because the clay interlayer distance increased from 2.47 nm ($2\theta = 3.5°$) to 3.9 nm ($2\theta = 2.3°$). Surprisingly, two different morphologies were observed together in the HPP/Cloisite 20A sample compatibilized with $PPgIA_{0,7}$, because some clay sheets got closer to each other, as shown

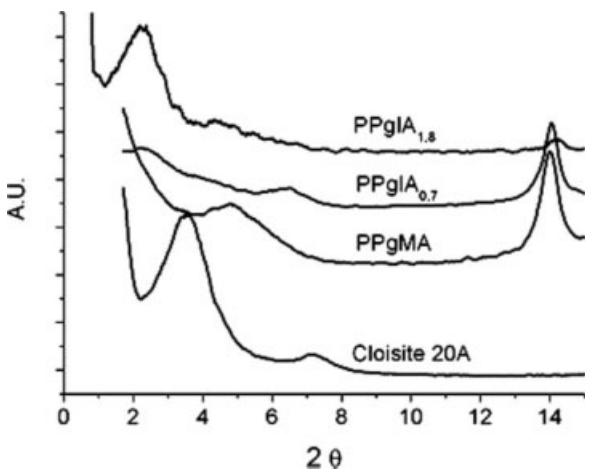

Figure 5 XRD patterns of the HPP/Cloisite 20A composites containing 5 wt % of clay with different types of compatibilizers.

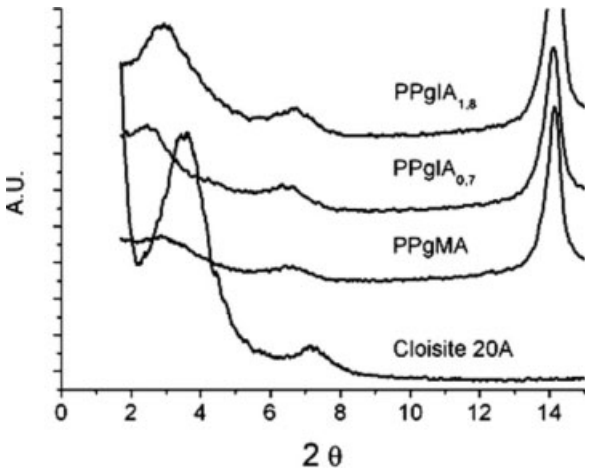

Figure 6 XRD patterns of the PP/Cloisite 20A composites containing 5 wt % of clay with different types of compatibilizers.

by the small peak around $2\theta = 6.4°$, but other sheets are intercalated and their peak is shifted to lower 2θ values, around $2\theta = 2.3°$ (3.9 nm). This split in the interlayer distance has already been reported in some polymer/clay nanocomposites.[19] It is noteworthy that because no other peak appears at an angle related to those of the collapsed clays (for example, in the half value for the d_{002} peak), it is believed that these peaks are not associated with some secondary diffraction coming from intercalated clays with interlayer distances that are out of range of the X-ray equipment.[18] Moreover, the HR-TEM images showed interlayer distances similar to those measured by XRD in composites with clay collapse (see below).

Therefore, it is clear from our results that the final morphology of the HPP/clay composites, in particular their interlayer distance, depends not only on the type of clay and its organic modifier, but also on the specific compatibilizer used.

To analyze the effect of the polymer matrix on the clay's morphology, the X-ray diffraction patterns of the composites based on pure low molecular weight polypropylene were also studied using different compatibilizers and clays. The same as in the HPP matrix, clay collapse was seen in composites prepared with either O-Zl or O-KSF, and their interlayer distance decreased to about 1.38 nm ($2\theta = 6.2°$) regardless of the compatibilizer used. However, differences were found when Cloisite 20A was used, as seen in Figure 6. In this case, regardless of the kind of compatibilizer, all the composites showed both the intercalated and the collapsed states together. Therefore, the matrix affects the polymer/clay morphology[29,30] and, as already reported, polypropylenes with low molecular weights present better interactions with OLSs.[29,30]

Stability of organically modified clays

As mentioned earlier, clay collapse can be associated with two different mechanisms: changes in the morphology of its organic molecules from mono- to bilayer structure, or thermal degradation together with water release processes due to the high temperatures used for the preparation of nanocomposites.[26] To verify if under the processing conditions the clay undergoes either water release or degradation of the intercalated organic molecules, the thermal stability of the OLSs was studied by diffuse reflectance spectroscopy (DRIFT) at 190°C as a function of time. Figure 7 shows the DRIFT spectra at 190°C for Cloisite 20A at times between 0.5 and 12 min. The DRIFT spectra were also recorded at room temperature. The results for both the O-Zl and the O-KSF samples are not shown because they were entirely similar. Surprisingly, the absorption bands associated with the presence of organic molecules (around 2900 and 1500 cm^{-1}) did not present any change under the conditions studied. Moreover, the absorption bands related to water molecules (around 3500 and 1650 cm^{-1}) were stable, so both possible processes are not relevant in the clays.

To confirm the absence of the degradation associated with the organic molecules of the OLSs, a thermogravimetric analysis (TGA) was performed. Figure 8 shows the TGA results for the O-KSF, O-Zl, and Cloisite 20A samples. It is seen that the water content of both O-KSF and O-Zl is around 2 wt %, so its presence is not relevant. Moreover, these values confirm the thermal stability of the samples under the operating conditions, because degradation temperature is always much higher than 190°C.

It is clear that the data obtained from Figure 8 are measured in a dynamic state, which is different

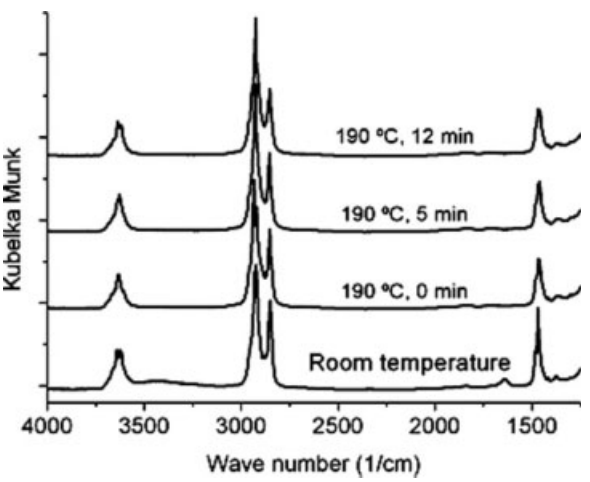

Figure 7 DRIFT spectra of Cloisite 20A at room temperature and after different times at 190°C. See text for signal assignment.

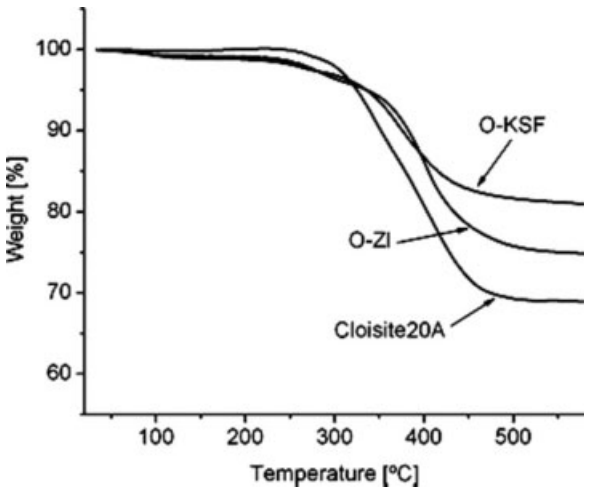

Figure 8 TGA analysis of different organically modified clays.

from the melt-mixing conditions, so TGA was also made at constant temperature, 190°C. The results agree with the DRIFT measurements, because no relevant degradation is seen after 60 min, and only 2.5% weight loss is detected.

So from the results of DRIFT and TGA, it is possible to conclude that the decrease in the interlayer distance is not associated with either the degradation of organic molecules or water loss. Moreover, the possible degradation of organic molecules in the clay was further studied by increasing the mixing time used for the preparation of the master batch. No substantial change was observed in the interlayer distance of the clays, even for mixing times longer than 30 min. On the other hand, a comparison was made of the interlayer distance of the O-KSF clay after treatment at 190°C in a vacuum oven. After 10 min (the time elapsed in the melt-mixer), no change was found in the gallery heights. The same behavior was seen with O-Zl. It is worth noting that the interlayer distance of Cloisite 20A remains stable after 6 h at 190°C. Thus, the presence of neat polymer is necessary to detect the clay collapse. It is also possible that due to the shear processes in the mixer the local temperature of the sample may have gone

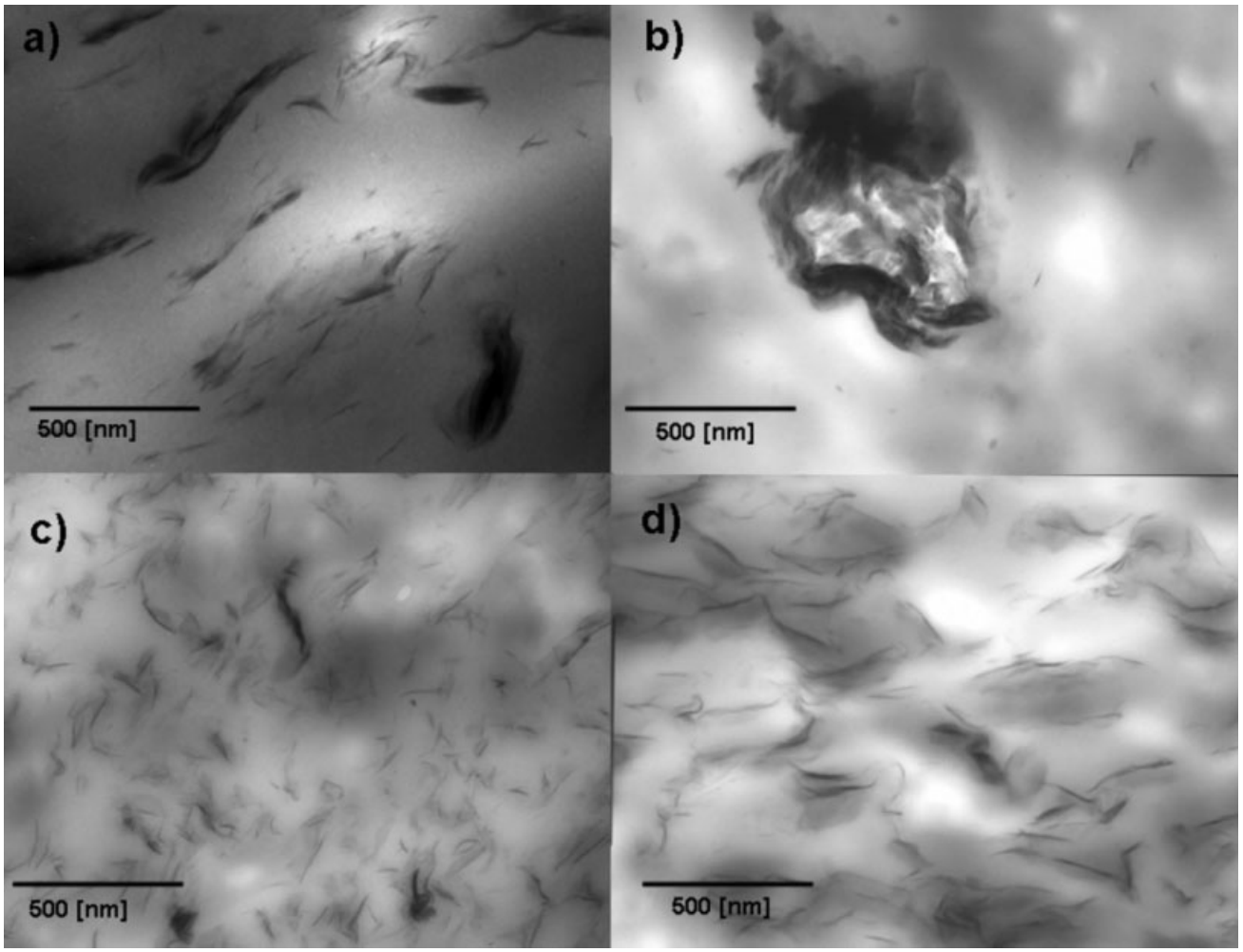

Figure 9 TEM images of some HPP composites with 5 wt % of filler using: (a) the O-Zl/PPgIA$_{1.8}$ system; (b) the O-KSF/PPgIA$_{0.7}$ system; (c) the Cloisite 20A/PPgMA system; and (d) the Cloisite 20A/PPgIA$_{0.7}$ system.

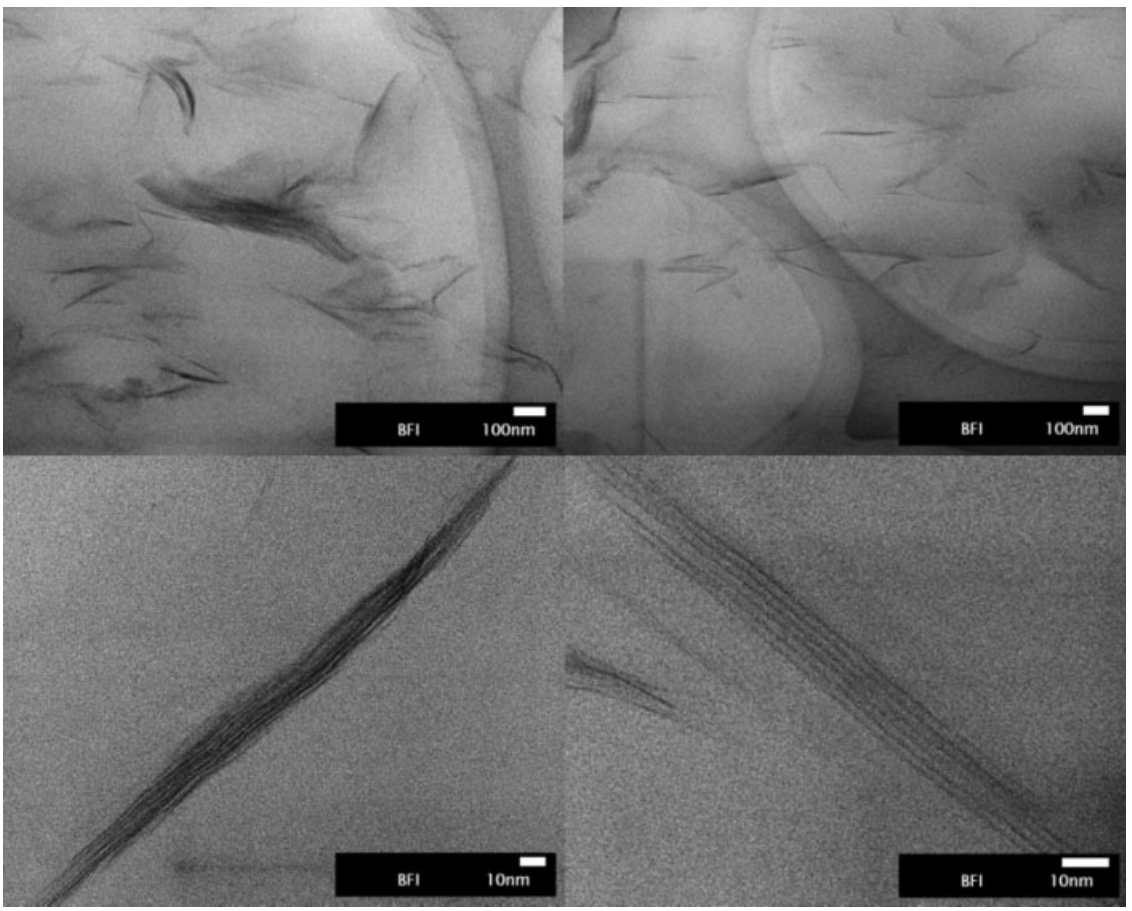

Figure 10 HR-TEM images of the PP/Cloisite 20A composites compatibilized with $PPgIA_{1.8}$.

above 190°C and new phenomena could appear that favor the degradation. Therefore, some composites were prepared by a solution process at 120°C using xylene as the solvent. However, the same trend was found, meaning that some samples presented clay collapse that rules out the last explanation.

TEM characterization

It is well known that the XRD is a good tool for evaluating clay morphology, in particular its interlayer distance. However, TEM is also needed to assess the overall state of the clay. Figure 9 shows TEM images of some HPP composites with 5 wt % of clay loading. In agreement with what was found by XRD measurements, the composite morphology depends on the clay used. The TEM images of the HPP/O-Zl and the HPP/O-KSF composites showed tactoid or immiscible clay particles, so that the clay collapse studied by XRD is associated with these immiscible particles. On the other hand, depending on the specific OLS/compatibilizer system used, together with collapsed tactoid particles, it is possible to see some degree of dispersion in the polymerc matrix, as can be seen in Figure 9(a).[31,32] These images also show that some clays were fractured.[33] With respect to the HPP/Cloisite 20A composites, in agreement with the XRD results, these samples showed better dispersion in the HPP matrix than the other clays, as seen in Figure 9(c,d), although with some amount of immiscible particles, which could account for the double morphology found by XRD.

On the other hand, Figure 10 shows HR-TEM images of the PP/Cloisite 20A composite when $PPgIA_{1.8}$ is used as compatibilizer. This sample presents both the intercalated and the collapsed state by X-ray analysis, and from Figure 10 it is also possible to observe two kinds of morphologies: good clay dispersion together with tactoid or immiscible structures. However, HR-TEM leads to the conclusion that no exfoliated state is found, but there are very well dispersed multilayer stacks about 10 nm thick which mean five silicate sheets per stack, similar to what has been reported for other clay nanocomposites.[31] The PP/O-KSF sample compatibilized with the PPgMA, which presented a clay collapse by XRD, shows tactoid or immiscible morphology, as seen in Figure 11. In this case multilayer stacks are agglomerated together and they are not dispersed as in other samples. Moreover, from these images it is

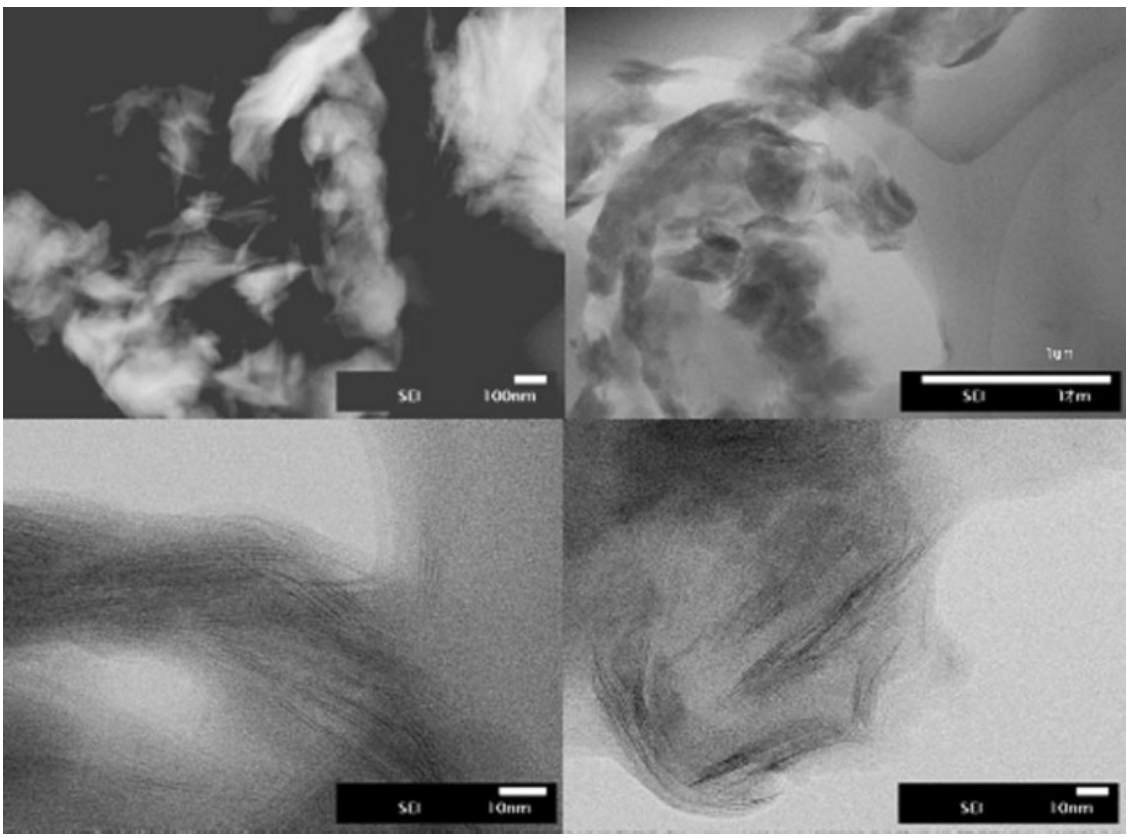

Figure 11 HR-TEM images of the PP/O-KSF composites compatibilized with PPgMA.

possible to estimate the interlayer distance of the immiscible structures and a value of 1.4 nm was found, which is close to that measured for collapsed clays by XRD, confirming that the collapsed state comes from these immiscible particles. From the last TEM results, it is clear that the OLS/compatibilizer system is the fundamental variable to understand the morphology of polypropylene/clay composites.

In spite of the different morphologies found in the composites, it is possible to conclude that by the addition of an OLS and a compatibilizer, the melt-processing was able to break up the original agglomerated clay particles, whose initial size was about 15 μm, into their primary size of less than 1 μm. This reduction in clay size is important for some of the composite's properties, for example, those related to its degradation processes, because it has been reported that not only completely exfoliated systems are able to change the properties of polymer matrices.[34–36] The latter will be evaluated in a coming contribution.

With respect to the samples with both morphologies observed at the same time by either XRD or TEM images, it is possible to understand this behavior by means of the distribution of CEC values within the clays. An isomorphic substitution[14,26] is a stochastic process, so it is possible to find galleries within a clay with either higher or lower CEC values than the experimental ones. Therefore, some galleries will interact with a polymer and they can be either exfoliated or intercalated; but others will not be able to do so. These galleries can feel the normal forces coming either from the layers that are intercalated or from the polymer molecules that surround them, and in this way the galleries may collapse. Moreover, it has been reported that the clay's collapse is due to the change in the interlayer structure of the organic molecules from bi- to mono-layer morphology,[18] and it is, therefore, possible to think that the normal forces on the collapsed layers can catalyze this process.

CONCLUSIONS

Different types of compatibilizers and clays were used for the preparation of polypropylene/clay nanocomposites in which it was found that the clays with the lowest CEC value and modified with ODA presented a decrease in the interlayer distance associated with the clay collapse. However, an important intercalated state was seen in clays with the highest CEC and organically modified with a set of quaternary ammonium salts. Moreover, depending on the compatibilizer used, some samples presented both the morphologies together. The decrease in the interlayer distance found in some samples is not

associated with the degradation of organic molecules from the clays, as seen from DRIFT and TGA.

On the other hand, high-resolution TEM confirmed that, depending on both the clay and the compatibilizer used, several morphologies can be obtained. Clays showing collapsed morphology by XRD presented immiscible structures, but those clays with intercalated states presented well dispersed multilayer stacks about 10 nm thick.

It is concluded that the OLS/compatibilizer system as a whole affects the morphology of composites better than the OLS by itself.

The supply of the polypropylenes by Petroquímica Cuyo S.A. and Petroquim S.A. is gratefully acknowledged. We express our thanks to Dr. F. Gracia and Dr. P. Araya for the DRIFT measurements, and to Dr. W. Sierralta for the TEM images and to the International Center for Young Scientists (ICYS)/National Institute for Material Science (NIMS), Tsukuba-Japan, for the HR-TEM images.

References

1. Thostenson, E.; Li, C.; Chou, T. Comp Sci Tech 2005, 65, 491.
2. Jordan, J.; Jacob, K.; Tannenbaum, R.; Sharaf, M.; Jasiuk, I. Mater Sci Eng A 2005, 393, 1.
3. Moniruzzaman, M.; Winey, K. Macromolecules 2006, 39, 5194.
4. Coleman, J.; Khan, U.; Gun'ko, Y. K. Adv Mater 2006, 18, 689.
5. Goettler, L. A.; Lee, K. Y.; Thakkari, H. Polym Rev 2007, 47, 291.
6. Samir, M.; Alloin, F.; Dufresne, A. Biomacromolecules 2005, 6, 612.
7. Ray, S.; Okamoto, M. Prog Polym Sci 2003, 28, 1539.
8. Winey, K.; Vaia, R. MRS Bull 2007, 32, 314.
9. Balazs, A.; Emrick, T.; Russell, T. P. Science 2006, 314, 1107.
10. Termonia, Y. Polymer 2007, 48, 6948.
11. Usuki, A.; Kawasumi, Y.; Kojima, M. J Mater Res 1993, 8, 1179.
12. Vaia, R.; Giannelis, E. Macromolecules 1997, 30, 8000.
13. Kawasumi, M.; Hasegawa, N.; Kato, M.; Usuki, A.; Okada, A. Macromolecules 1997, 30, 6333.
14. Manias, E.; Touny, A.; Wu, L.; Strawhecker, K.; Lu, B.; Chung, T. C. Chem Mater 2001, 13, 3516.
15. Nam, P.; Maiti, P.; Okamoto, M.; Kotaka, T.; Hasegawa, N.; Usuki, A. Polymer 2001, 42, 9633.
16. Kim, K. N.; Kim, H.; Lee, J. W. Polym Eng Sci 2001, 41, 1963.
17. Benetti, E. M.; Causin, V.; Marega, C.; Marigo, A.; Ferrara, G.; Ferraro, A.; Consalvi, M.; Fantinel, F. Polymer 2005, 46, 8275.
18. Yoon, J.; Jo, W.; Lee, M.; Ko, M. Polymer 2001, 42, 329.
19. Pozsgay, A.; Fràter, T.; Szazdi, L.; Muller, P.; Sajo, I.; Pukanszky, B. Eur Polym J 2004, 40, 27.
20. Zanetti, M.; Camino, G.; Reichter, P.; Mulhaupt, R. Macromol Rapid Commun 2001, 22, 176.
21. He, A.; Hu, H.; Huang, Y.; Dong, J.; Han, C. Macromol Rapid Commun 2004, 25, 2008.
22. Su, S.; Wilkie C. Polym Degrad Stab 2004, 83, 347.
23. March, J. Advanced Organic Chemistry, 1st ed.; McGraw-Hill Kogakusa Ltd: Tokyo, 1977.
24. Bruna, J.; Yazdani-Pedram, M.; Quijada, R.; Valentín, J. L.; López-Manchado, M. A. React Funct Polym 2005, 64, 169.
25. Yazdani-Pedram, M.; Vega, H.; Quijada, R. Polymer 2001, 42, 4751.
26. Madejota, J. Vib Spectrosc 2003, 31, 1.
27. Vaia, R.; Teukolsky, R.; Giannelis, E. Chem Mater 1994, 6, 1017.
28. Maiti, P.; Yamada, K.; Okamoto, M.; Ueda, K.; Okamoto, K. Chem Mater 2002, 14, 4654.
29. Moncada, E.; Quijada, R.; Retuert, J. J Appl Polym Sci 2006, 103, 698.
30. Gianelli, W.; Ferrara, G.; Camino, G.; Pellegatti, G.; Rosenthal, J.; Trombini, J. C. Polymer 2005, 46, 7037.
31. Sheng, N.; Boyce, M. C.; Parks, D. M.; Rutledge, G. C.; Abes, J. I.; Cohen, R. E. Polymer 2004, 45, 487.
32. Brown, J. M.; Curliss, D.; Vaia, R. A. Chem Mater 2000, 12, 3376.
33. Weon, J. I.; Sue, H. J. Polymer 2005, 46, 6325.
34. Qin, H.; Zhang, S.; Zhao, C.; Yang, M. J Polym Sci Part B: Polym Phys 2005, 43, 3713.
35. Causin, V.; Marega, C.; Marigo, A.; Ferrara, G.; Ferraro, A.; Selleri, R. J Nanosci Nanotechnol 2008, 8, 1823.
36. Qin, H.; Zhang, S.; Zhao, C.; Feng, M.; Yang, M.; Shu, Z.; Yang, S. Polym Degrad Stab 2004, 85, 807.